INSTITUTE OF PHYSICS PUBLISHING NANOTECHNOLOGY

Nanotechnology **16** (2005) 1630–1635 doi:10.1088/0957-4484/16/9/038

Modified self-assembly of InAs islands acting as stressors for strain-induced InGaAs(P)/InP quantum dots

J Sormunen[1], **J Riikonen, M Mattila, M Sopanen and H Lipsanen**

Optoelectronics Laboratory, Helsinki University of Technology, PO Box 3500, FIN-02015 HUT, Finland

E-mail: jaakko.sormunen@hut.fi

Received 19 April 2005, in final form 2 June 2005
Published 1 July 2005
Online at stacks.iop.org/Nano/16/1630

Abstract

We report modified self-assembly of InAs islands acting as stressors for strain-induced InGaAs(P) quantum dots (SIQDs). The quantum dots are fabricated by growing InAs islands on top of a near-surface InGaAs(P)/InP quantum well (QW). The compressively strained QW affects the size and density of the InAs islands, as compared to islands grown on a plain InP buffer. By adjusting the growth conditions, the height of the InAs stressors is tuned from 15 to 30 nm while the areal density varies around 10^9 cm^{-2}. The confinement of carriers in the SIQDs is characterized by low-temperature photoluminescence. Increasing the size of the InAs stressor is shown to enhance the depth of the lateral confinement potential and reduce the level splitting of excited QD states. However, the small inhomogeneous broadening of the SIQD transitions, as narrow as 11 meV, shows no correlation with the height dispersion of the stressor islands.

1. Introduction

Coherent Stranski–Krastanov (SK) growth has been widely applied in the fabrication of low-dimensional semiconductor nanostructures. Recent examples are InAs quantum dots (QDs), used in, e.g., lasers [1] and all-optical switches [2] operating around 1.5 μm, and resonant tunnelling structures [3]. Typically, such QD devices consist of self-assembled InAs islands buried in a barrier material with a higher band gap, such as InP, GaAs, or InGaAsP. An alternative way to create QDs, however, is to use the self-assembled islands as stressors [4]. The tensile strain underneath the islands is utilized to locally reduce the band gap of a near-surface quantum well (QW). The resulting lateral confinement potential is nearly parabolic for both electrons and holes, and the vertical confinement is achieved by the high-quality interfaces of the QW. The versatility of this approach is that the emission wavelength of the strain-induced quantum dots (SIQDs) can be tuned by adjusting the QW composition, virtually independently of the stressor islands. Furthermore, SIQDs provide an interesting means to study the physics of nearly perfect quantum dots [5], especially as the strain and the induced confinement potential can be modelled in a straightforward manner [6].

Self-assembled SIQDs were first implemented in the InGaAs/GaAs material system, using InP islands as stressors [7]. Subsequently, GaInNAs/GaAs, GaInP/AlGaInP, GaAs/AlGaAs, and SiGe/Si SIQDs have been fabricated [8–11]. However, InGaAs/InP SIQDs [12] have been demonstrated only recently, utilizing InAs stressor islands. The important advantage of the InP-based material system is the possibility of using lattice-matched InGaAsP in the QW. This offers a wide tuning range for the wavelength of the SIQD structure, spanning for example the regions of 1.3 and 1.55 μm.

In this paper, we study the effect of InAs stressor islands on both ternary InGaAs/InP and quarternary InGaAsP/InP SIQDs. The size and areal density of the islands are varied by adjusting the growth temperature and nominal InAs coverage. As compared to case for InAs islands grown on plain InP, the compressively strained near-surface QW is observed to affect the island self-assembly. Low-temperature photoluminescence (PL) is used to study the influence of

[1] Author to whom any correspondence should be addressed.

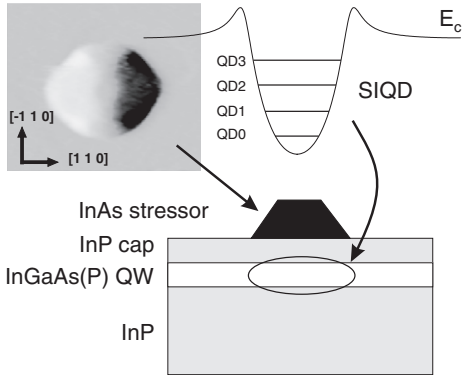

Figure 1. Layer structure of the SIQD sample. The insets show an AFM image of a typical InAs island (top left) and the schematic deformation of the conduction band edge in the InGaAs QW (top right).

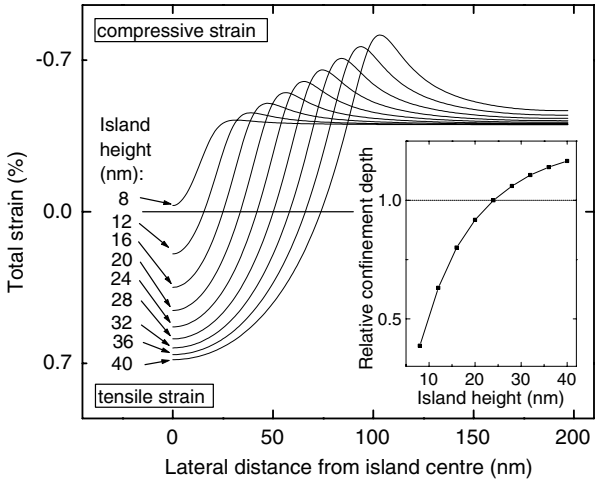

Figure 2. Calculated total strain in the InGaAs QW under the InAs stressor island as a function of lateral (radial) distance. The inset shows the relative depth of the lateral confinement potential as a function of island height.

the size of the islands on the optical properties of the induced quantum dots and the experimental data are compared to computational strain calculations. Moreover, the size distribution of the InAs stressor islands is compared to the inhomogeneous broadening of the QD PL. The observed growth-related phenomena are discussed in terms of As/P exchange and the strain energy of the stressor/substrate system.

2. Experimental details

The samples were fabricated by metal–organic vapour phase epitaxy (MOVPE) in a horizontal quartz-glass reactor under atmospheric pressure. Hydrogen was used as the carrier gas while utilizing trimethylindium (TMI), trimethylgallium (TMG), tertiarybutylphosphine (TBP), and tertiarybutylarsine (TBA) as precursors. The epitaxial layers were grown on Fe-doped semi-insulating InP(001) wafers. Prior to deposition, the substrates were annealed for 5 min at 650 °C after which a 100 nm thick InP buffer layer was grown at 640 °C. Subsequently a compressively strained 10 nm quantum well, either $In_{0.59}Ga_{0.41}As$ or $In_{0.68}Ga_{0.32}As_{0.83}P_{0.17}$, and a 7 nm InP capping layer were grown, also at 640 °C. The stressor islands were then fabricated by depositing 0.65−1.7 monolayers (MLs) of InAs during the first few seconds of a temperature ramp-down from the growth temperature of 550–570 °C. The temperature was ramped down already during the growth of the islands in order to reduce the effects of As/P exchange [13–15], such as the uncontrolled accumulation of excess material into the islands after deposition. Compared to growth at a constant temperature [16], this procedure was found to result in more homogeneous islands and is further discussed below. It should be noted that in this text, the growth temperature of the islands refers to the nominal temperature before the ramp-down step.

The surface morphology of all the samples was captured *ex situ* by contact-mode atomic force microscopy (AFM). Island density and height information were extracted from $3\times3\ \mu m^2$ AFM scans. The photoluminescence measurements were conducted at 10 K, utilizing a diode-pumped frequency-doubled Nd:YVO_4 laser emitting at 532 nm for excitation. A liquid-N_2-cooled germanium detector and standard lock-in techniques were used to record the PL spectra.

3. Results and discussion

The structure of the SIQD samples is shown in figure 1. Top right, the modulation of the QW conduction band edge and discrete energy levels of the quantum dot are shown schematically. A top-view AFM image of an InAs island, 26 nm in height and with a 130 nm base diameter, is also shown. The lateral dimension may be slightly exaggerated due to the finite curvature of the AFM tip. Therefore, in this work, the size of the islands is characterized by their height. On the basis of the AFM data, the typical aspect ratio (height/base diameter) of the InAs islands is approximately 0.2.

First, to estimate the influence of the size of the InAs island to the SIQD confinement potential, the finite element method (FEM) was used to computationally solve for the strain induced by the stressor (see [6]). The height h of the island was varied between 8 and 40 nm while keeping the aspect ratio constant at 0.2. Figure 2 shows plots of the total strain in the middle of the $In_{0.59}Ga_{0.41}As$ quantum well under the stressors of different size. Because the band-edge deformation depends linearly on the strain components, the depth of the lateral confinement potential is proportional to the strain difference between the centre of the island and far away from the island. The inset of figure 2 shows the relative confinement depth as a function of stressor height, normalized to 1 at $h = 24$ nm. The confinement depth declines rapidly as the height of the stressor decreases below 15 nm. Thus, islands much smaller than that are unlikely to induce quantum dots with high quantization. On the other hand, above 30 nm, the depth of confinement increases only somewhat and the islands may also become non-coherent. Therefore, this paper focuses on stressor islands in the height scale from 15 to 30 nm.

Next, the influence of the quantum well on the self-assembly of the InAs islands was investigated. 1.3 and 1.7 ML of InAs were deposited both directly on an InP buffer (set A) and on the capping layer of an InGaAs/InP near-surface QW (set B). During growth, the temperature was ramped down from 550 °C, as described above. For comparison, samples

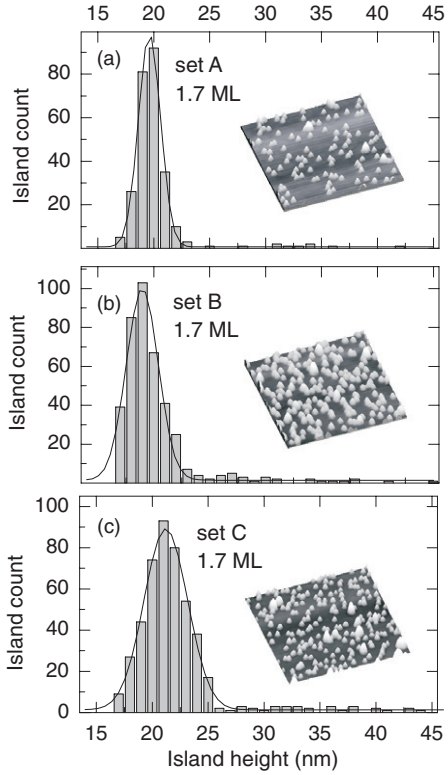

Figure 3. Height distribution histograms of InAs islands grown on (a) plain InP buffer (set A), (b) near-surface InGaAs QW (set B) with the ramp-down procedure, and (c) near-surface QW at a constant temperature (set C). The insets show the corresponding 2×2 μm^2 AFM images with a vertical scale of 40 nm.

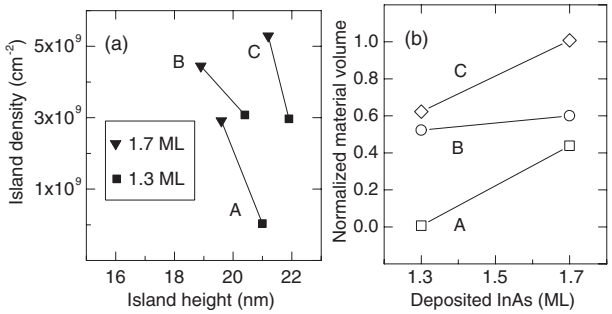

Figure 4. (a) Areal density of InAs islands grown on plain InP buffer (set A), near-surface InGaAs QW (set B), and near-surface QW at a constant temperature (set C), plotted against average island height. (b) Normalized material volumes in the InAs islands plotted as a function of deposited InAs coverage in sets A, B, and C.

similar to set B were grown at a constant growth temperature of 550 °C (set C). Figure 3 shows height histograms of InAs islands (1.7 MLs) from the sets (a) A, (b) B, and (c) C. The insets show the corresponding 2×2 μm^2 AFM images. In figure 4(a), the areal density of the islands is plotted as a function of average island height. It is observed that with increasing InAs coverage, the island density increases and the height somewhat decreases. This is an expected result and is due to an increased supersaturation at the onset of nucleation which leads to a higher nucleation density [17]. Interestingly, the areal density is notably lower for islands grown on plain InP (set A) as compared to islands grown on the near-surface QW. In set A, a deposition of 1.3 ML is just above the critical limit for island formation. This implies that the threshold for the 2D–3D transition may be lowered by the strain of the QW in sets B and C. In figure 4(b), the total material volumes in the InAs islands, calculated from the AFM data, are plotted as a function of nominal InAs coverage. The islands grown on plain InP have accumulated less material than the islands grown on the near-surface QWs. Although this may be partly due to a thicker wetting layer in set A, it is likely that most of the extra material in sets B and C comes from the exposed InP surface through As/P exchange [16] which may be further enhanced by strain [18].

Comparing sets B and C in figures 4(a) and (b), it is noted that while the island densities are approximately the same, the average island size is larger in set C. Furthermore, the material volumes are higher in C. It is concluded that this must be due to a difference in the rate of As/P exchange during the growth of the islands. Group V exchange before the nucleation of the islands affects mainly the nucleation density through an increase in supersaturation. Therefore, similar island densities imply that the growth conditions before the nucleation are close to identical in the ramp-down process and growth at a constant temperature. However, after nucleation, the ramp-down procedure results in a diminished As/P exchange which is seen as a decrease in the excess material accumulated in the islands. Simultaneously, the full width at half-maximum (FWHM) of the island height distribution drops from 3.9 to 3.1 nm (at 1.7 ML), as determined by fitting Gaussian profiles to the histogram data (figures 3(b) and (c)). Thus, the homogeneity of the island ensemble is improved, presumably due to a suppression of As/P exchange during the nucleation phase which is thereby shortened. Decreasing the nominal InAs coverage to 0.8 ML narrowed the height FWHM further to 2.2 nm.

To fabricate stressors of various sizes, the growth temperature of the islands was varied. Figure 5 shows height histograms of InAs islands (0.8 ML) grown at (a) 570 °C, (b) 560 °C, and (c) 550 °C. The insets in figure 5 show the 2×2 μm^2 AFM images of the corresponding samples. The island mean height and FWHM increase from 18.8 nm and 2.2 nm at 550 °C to 28.8 nm and 5.3 nm at 570 °C, respectively. Thus, the ensemble of larger islands grown at a higher temperature is slightly less homogeneous than that grown at a lower temperature.

In order to further vary the size and distribution of the stressors, nominal InAs coverages of 0.65 and 1.0 ML were also deposited. Figure 6 shows the areal density of InAs islands plotted against average height, grown at 550, 560, and 570 °C with varying deposition thickness. The stressor height is noted to increase with temperature regardless of the deposition thickness. As a general trend, the island density and height are inversely proportional. This is a consequence of mass distribution [19]: because the density of nucleated islands decreases with increasing temperature [17], the deposited material is distributed over fewer islands at higher temperatures. However, with a deposition thickness of 0.65 ML, the InAs island density increases with increasing temperature. This behaviour may be explained by acknowledging that the nominally deposited

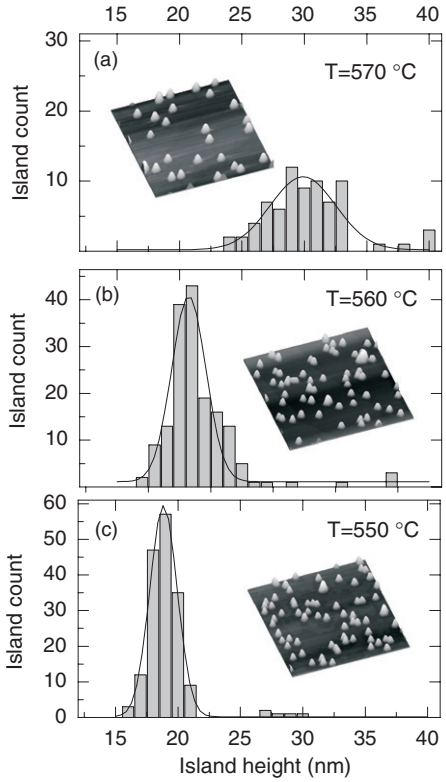

Figure 5. Height distribution histograms of InAs stressor islands grown at (a) 570, (b) 560, and (c) 550 °C. The insets show the corresponding 2 × 2 μm^2 AFM images with a vertical scale of 40 nm.

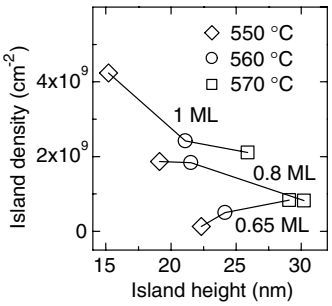

Figure 6. Areal density of InAs stressor islands plotted against average height. The figure shows samples grown at 550, 560, and 570 °C with different InAs deposition thicknesses (0.65–1.0 ML).

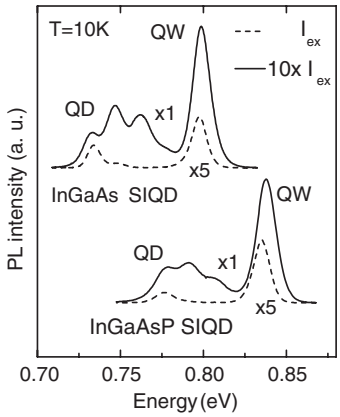

Figure 7. PL spectra of InGaAs and InGaAsP SIQD samples measured at low (dashed lines) and high (solid lines) excitation intensity.

thickness here is well below the critical limit for the 2D–3D transition [20], and the rest of the material needed comes from the interface through As/P exchange. Raising the temperature increases the rate of exchange [13] which in turn amounts to a higher supersaturation at the onset of nucleation. Hence, the nucleation density is increased.

In addition to affecting the nucleation, the As/P exchange was also shown to affect the growth of the islands. To estimate the amount of incorporated 'exchanged' material, the total material volumes in the islands were calculated from the AFM data (not shown here). It was noted that with a fixed deposition thickness, raising the growth temperature distinctly increased the volume in the islands. At 570 °C, the material volumes were typically more than twice as high as at 550 °C. Three conclusions are drawn from this:

(i) Material accumulated from the interface through As/P exchange seems to account to more than half of the material in the islands grown at 570 °C.
(ii) With the exchanged (In)As, also some of the released (In)P might be re-incorporated into the islands, thus forming InAsP [19]. This alloying would obviously diminish the strain effect of the stressor.
(iii) The effect of excess material accumulation could be drastically reduced by lowering the temperature.

However, this would also lead to a reduction in the size of the islands which is an undesired effect. Ideally, the temperature should be high enough during nucleation to ensure the right density of coherent islands but low enough during the subsequent growth of the islands to reduce the As/P exchange effects. This again motivates the use of the temperature ramp-down during InAs deposition.

To characterize the effects of the stressor islands on the QD energy state structure, PL was measured from nine SIQD samples with a near-surface InGaAs quantum well and InAs stressors whose average height was varied between 15 and 30 nm. For reference, another set of three SIQD samples with a quarternary InGaAsP QW was measured. In figure 7, PL spectra from InGaAs and InGaAsP SIQD samples with InAs islands grown at 560 °C are shown. At low excitation intensity (dashed lines), both samples mainly show luminescence from the QW and the quantum dot ground state (QD0). In the InGaAs sample, the QD0 peak at 0.733 eV is redshifted by 66 meV from the QW peak. Meanwhile, the InGaAsP QW luminesces at 0.838 eV and the corresponding QD0 peak is redshifted by 61 meV. At a higher excitation intensity (solid lines), both samples show state filling, i.e., luminescence from higher SIQD states (QD1–QD3) emerge as lower states become fully populated [5, 12]. By fitting Gaussian profiles to the spectra shown, the level splittings between consecutive QD states were resolved as 14.1–15.0 meV (InGaAs QDs) and 14.7–15.6 meV (InGaAsP QDs). The almost equal separation between different states is attributed to the nearly parabolic confinement potential and the corresponding level splitting $\hbar\omega$ of the harmonic oscillator.

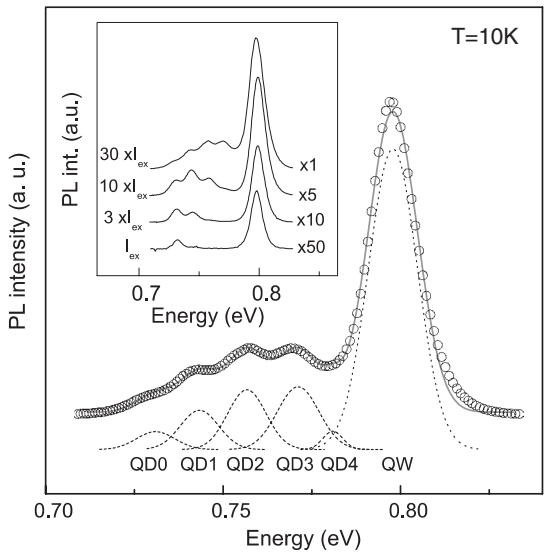

Figure 8. Gaussian profiles fitted to a PL spectrum measured from SIQD sample with stressors of 29 nm mean height. Five fitted SIQD peaks and the QW peak are shown with dotted lines. The measured PL spectrum (open circles) and the fitted curve (solid line) are offset vertically for clarity. The inset shows PL spectra measured from the same sample with various excitation intensities (I_{ex}).

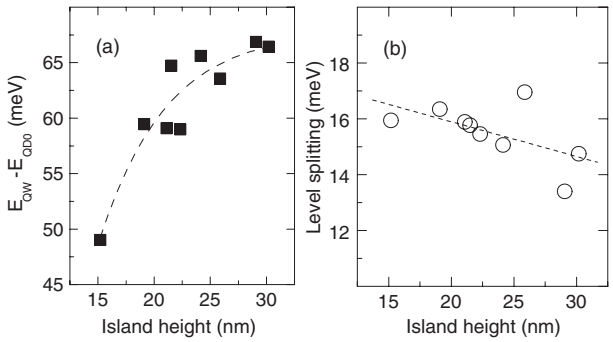

Figure 9. (a) Redshift of the QD0 PL peak from the InGaAs QW peak as a function of island height (filled rectangles). The fitted curve (dashed line) is shown as a guide for the eye. (b) Average level splitting of the InGaAs SIQD states as a function of stressor height (open circles). The dotted line is a linear fit to the data.

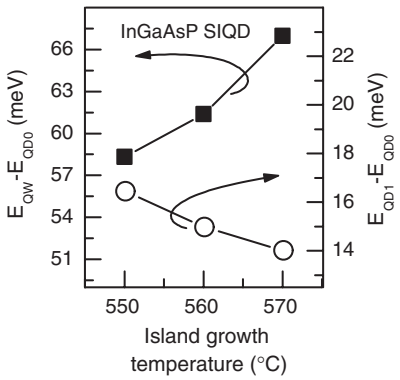

Figure 10. Redshift of the InGaAsP QD0 PL peak from the InGaAsP QW peak (black rectangles) and separation of InGaAsP QD1 and QD0 peaks (open circles) plotted as a function of stressor growth temperature.

The InGaAs QD level splitting was also calculated with a simple 2D rotationally symmetric potential corresponding to the values obtained from the FEM strain calculations. Using $m^* = 0.033\ m_0$ for electrons and $m^* = 0.049\ m_0$ for lateral 'heavy' holes, we obtained a level splitting of 15 meV in which $\hbar\omega_e = 11$ meV and $\hbar\omega_{hh} = 4$ meV. The calculated redshift was 61 meV of which 49 meV originated from the conduction band side. These values are close to the experimental results and more detailed calculations are to be published elsewhere.

The largest QD0 redshift, 67 meV, was measured from the InGaAs SIQD sample with InAs islands (0.65 ML) grown at 570 °C. Figure 8 shows the PL spectrum of the sample (open circles), measured at a high excitation intensity, along with Gaussian profiles fitted to QD transitions QD0–QD4 and the QW peak (dashed lines). The fitted sum curve (solid line) is a good match to the measured data. The inset in figure 8 shows PL spectra of the same sample at various excitation intensities, illustrating the progress of state filling.

It was already shown that, according to computation, increasing the size of the InAs stressor island deepens the confinement potential. To verify this, QD0 PL redshifts measured from InGaAs SIQD samples were plotted as a function of average island height, as presented in figure 9(a) with filled rectangles. The data show a clear correlation which is accentuated by the fitted curve (dashed line), drawn as a guide for the eye. The redshift increases with increasing island height but starts to saturate as the height approaches 30 nm. Comparing to the calculated relative confinement depth in the inset in figure 2, we see that there is a good agreement between the experimental behaviour and the strain calculations. In figure 9(b), the average level splitting of each InGaAs SIQD sample is plotted against stressor height (open circles). A linear fit to the data (dotted line) shows that with increasing island size, the separation between consecutive QD states is reduced. This can be explained by the fact that an increase in the stressor size increases the physical width of the confinement potential, as is seen also in figure 2. For comparison, the QD0 redshift and level splitting of the InGaAsP SIQD samples are shown in figure 10, plotted as a function of island growth temperature.

Finally, to study the homogeneity of the quantum dots, the linewidths of the QD PL transitions were extracted from the fitted Gaussian profiles. Figure 11 shows the FWHM of the InGaAs QD0 peaks plotted against the FWHM of the island height distribution from the respective samples. Curiously, there seems to be little or no correlation between the homogeneity of the stressor islands and the PL linewidth. The FWHM of the QD peaks varies between 11 and 17 meV and is about the same as the FWHM of the QW peak (13–21 meV). These observations and earlier results from InGaAs/GaAs SIQDs [4] indicate that the FWHM of the SIQD ensemble is mainly determined by the QW confinement along the growth (z) axis and no broadening due to inhomogeneity in the lateral confinement is observed. On the contrary, the QD peaks here are typically slightly narrower than the corresponding InGaAs/InP QW peak. This suggests that the strain fields inducing the QDs are in fact very homogeneous, despite the apparent stressor height inhomogeneity. In addition, as was already noted, the width of the strain potential affects the level

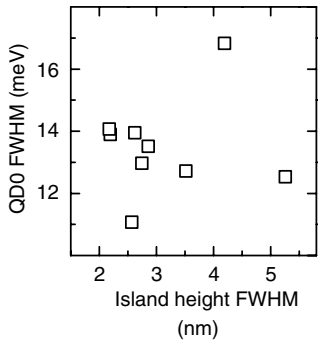

Figure 11. Full width at half-maximum (FWHM) values of InGaAs QD0 PL peaks plotted as a function of the FWHM of the island height distribution.

splitting of the QD states. Therefore, inhomogeneity of the stressor diameter would be expected to have a strong impact on the QD PL linewidth. However, because AFM does not provide very accurate data on island diameter, a more detailed investigation of possible correlation using, e.g., TEM should be conducted.

While discussing the stressor homogeneity, it should not be overlooked that the growth of the islands is affected not only by the kinetics, but also by thermodynamic effects, i.e., elastic energy, surface energy, and edge energy [21–24]. The elastic relaxation energy is the sum of the strain energy in the island and the strain energy induced by the island in the substrate and thus relates to the depth and shape of the SIQD confinement potential. It was already demonstrated that the strain field of the underlying near-surface QW can affect the island growth. Other reports have shown that the self-assembly of islands can be controlled by strain of the substrate [25] and that there are certain energetically favourable island sizes [26], associated with strain-induced growth hindrances. Therefore, if the strain energy governs the growth thermodynamics, the self-assembly of the islands may be linked to the uniformity of the strain fields of the stressors. Such linkage would provide some explanation to the remarkable homogeneity of the SIQD ensemble. However, the exact mechanism behind this phenomenon and how it relates to the height distribution of the islands remains a topic for further study.

4. Conclusions

In summary, the influence of InAs stressors on the properties of strain-induced InGaAs(P) quantum dots was studied by varying the islands fabricated on top of a compressively strained near-surface InGaAs(P)/InP quantum well. The strain field of the QW was shown to modify the self-assembly of the InAs islands by increasing the island density and reducing the amount of deposited InAs required for the 2D–3D transition. The depth of the carrier-confining potential was shown to increase as the height of the stressor was increased. Simultaneously, due to lateral broadening of the confinement potential, the average QD level splitting was reduced. Despite this dependence, the PL FWHM values, as narrow as 11 meV for the QD0 transition, were mainly limited by the linewidth of the quantum well peak. The stressor height uniformity and the QD PL linewidth showed no correlation. On the whole, it was demonstrated that the properties of InGaAs(P) quantum dots can be tuned by adjusting the InAs stressor islands and the composition of the quantum well. The tunability together with the excellent homogeneity of the QDs make this a promising material system for further investigation.

Acknowledgment

The authors thank Jukka Tulkki for his insight and help in the strain calculations.

References

[1] Caroff P, Platz C, Dehaese O, Paranthoën C, Bertru N, Corre A L and Loualiche S 2005 *J. Cryst. Growth* **278** 329–34
[2] Prasanth R *et al* 2004 *Appl. Phys. Lett.* **84** 4059
[3] Kamiya I, Tanaka I, Tada Y, Azuma M, Uno K and Sakaki H 2005 *J. Cryst. Growth* **278** 98–102
[4] Lipsanen H, Sopanen M and Ahopelto J 1995 *Phys. Rev.* B **51** 13868
[5] Grosse S, Sandmann J H H, von Plessen G, Feldmann J, Lipsanen H, Sopanen M, Tulkki J and Ahopelto J 1997 *Phys. Rev.* B **55** 4473
[6] Tulkki J and Heinämäki A 1995 *Phys. Rev.* B **51** 8239
[7] Sopanen M, Lipsanen H and Ahopelto J 1995 *Appl. Phys. Lett.* **66** 2364
[8] Koskenvaara H, Hakkarainen T, Lipsanen H and Sopanen M 2003 *J. Mater. Sci.* **14** 357
[9] Sopanen M, Taskinen M, Lipsanen H and Ahopelto J 1996 *Appl. Phys. Lett.* **69** 3393
[10] Wang T and Forchel A 1998 *Appl. Phys. Lett.* **73** 1847
[11] Kim E S, Usami N and Shiraki Y 1997 *Appl. Phys. Lett.* **70** 295
[12] Riikonen J, Sormunen J, Mattila M, Sopanen M and Lipsanen H 2005 *Japan. J. Appl. Phys.* **44** L518
[13] Wang B, Zhao F, Peng Y, Jin Z, Li Y and Liu S 1998 *Appl. Phys. Lett.* **72** 2433
[14] Gutiérrez H R, Cotta M A, Bortoleto J R R and de Carvalho M M G 2002 *J. Appl. Phys.* **92** 7523
[15] Poole P J, Williams R L, Lefebvre J and Moisa S 2003 *J. Cryst. Growth* **257** 89
[16] Taskinen M, Sopanen M, Lipsanen H, Tulkki J, Tuomi T and Ahopelto J 1997 *Surf. Sci.* **376** 60
[17] Seifert W, Carlsson N, Johansson J, Pistol M-E and Samuelson L 1997 *J. Cryst. Growth* **170** 39
[18] Yoon S, Moon Y, Lee T-W, Yoon E and Kim Y D 1999 *Appl. Phys. Lett.* **74** 2029
[19] Carlsson N, Junno T, Montelius L, Pistol M-E, Samuelson L and Seifert W 1998 *J. Cryst. Growth* **191** 347
[20] Cotta M A, Mendonca C A C, Meneses E A and Carvalho M M G 1997 *Surf. Sci.* **388** 84
[21] Moll N, Scheffler M and Pehlke E 1998 *Phys. Rev.* B **58** 4566
[22] Chen Y and Washburn J 1996 *Phys. Rev. Lett.* **77** 4046
[23] Wang L G, Kratzer P, Moll N and Scheffler M 2000 *Phys. Rev.* B **62** 1897
[24] Ponchet A, Corre A L, L'Haridon H, Lambert B, Salaün S, Alquier D, Lacombe D and Durand L 1998 *Appl. Surf. Sci.* **123/124** 751
[25] Yang B, Liu F and Lagally M G 2004 *Phys. Rev. Lett.* **92** 025502
[26] Reaves C M, Bressler-Hill V, Varma S, Weinberg W H and DenBaars S P 1995 *Surf. Sci.* **326** 209